2021

Motor Control System for Near-Resonance High-cycle Fatigue Testing

Samer K. Armaly
University of Central Florida

MOTOR CONTROL SYSTEM FOR NEAR-RESONANCE HIGH-CYCLE FATIGUE TESTING

by

SAMER ARMALY

A thesis submitted in partial fulfillment of the requirements
for the Honors in the Major Program in Aerospace Engineering
in the College of Engineering and Computer Science
and in the Burnett Honors College
at the University of Central Florida
Orlando, Florida

Spring Term

2021

Thesis Chair: Dr. Jeffrey L. Kauffman

ABSTRACT

This research project develops a low-cost high-cycle fatigue (HCF) testing system comprised of an AC motor, variable frequency drive (VFD), eccentric cam, and feedback controller. The system acts as a forced harmonic oscillator leveraging mechanical resonance to vibrate a specimen at a frequency required to induce the testing's strain amplitudes.

This system depends highly on the material being tested. As such, the controller incorporates material characteristics. A frequency sweep measures the strain amplitude to characterize the specimen. Additionally, other measurements such as acceleration can be used as a proxy control variables for strain. A function converts the control variable to frequency. This function tunes a proportional integral derivative (PID) controller to emphasize stable control. This function, coupled with a tuned PID controller, converts the correction update into a voltage signal that commands a motor speed to reach the desired strain amplitude.

Testing showed that a longer feedback loop time of 5 seconds was necessary to adequately control the system since the control variables are oscillatory by nature and need to be averaged over time to estimate accurate updates. Also, specimens with low damping are more subject to transient effects; consequently, rapid updates degrade system performance.

Overall, the system tested over 250,000 cycles and various specimens. The main limitation of the system is a maximum strain amplitude limited by the specific specimen resonant peak. However, adjusting the system’s fixed displacement enables transferring more force to the specimen, changing the shape of the resonant peak.

TABLE OF CONTENTS

LIST OF TABLES

List of Figures

NOMENCLATURE

AC = alternating current

DC = direct current

HCF = high-cycle fatigue

PID = proportional integral derivative (referring to a feedback controller)

SDOF = single degree of freedom

VFD = variable frequency drive

Variables

x = displacement

k = spring constant

c = damping constant

F = force

X = amplitude

ω = angular frequency

Φ = phase angle

ζ = damping ratio

E = Young's modulus

I = area moment of inertia

Subscripts

r = resonant

n = natural

0 = initial value

Superscript

$\cdot$ = time derivative

CHAPTER 1: INTRODUCTION

Fatigue testing is an essential aspect of designing a safe system and understanding material properties; understanding how a material behaves under repetitive strain is paramount to preventing catastrophic failures when used in critical systems. Unfortunately, critical systems such as fan blades in jet engines experience these effects. When these systems are not understood and characterized properly, uncontained engine failures can occur, as seen in recent incidents like the United flight 328 and Southwest flight 1380 uncontained engine failures. In these failures, high-speed fragments from stress fractures penetrated engine casings, destroying other integral parts of the system, As seen in Figure 1: Two fractured blades on the right engine Figure 1.

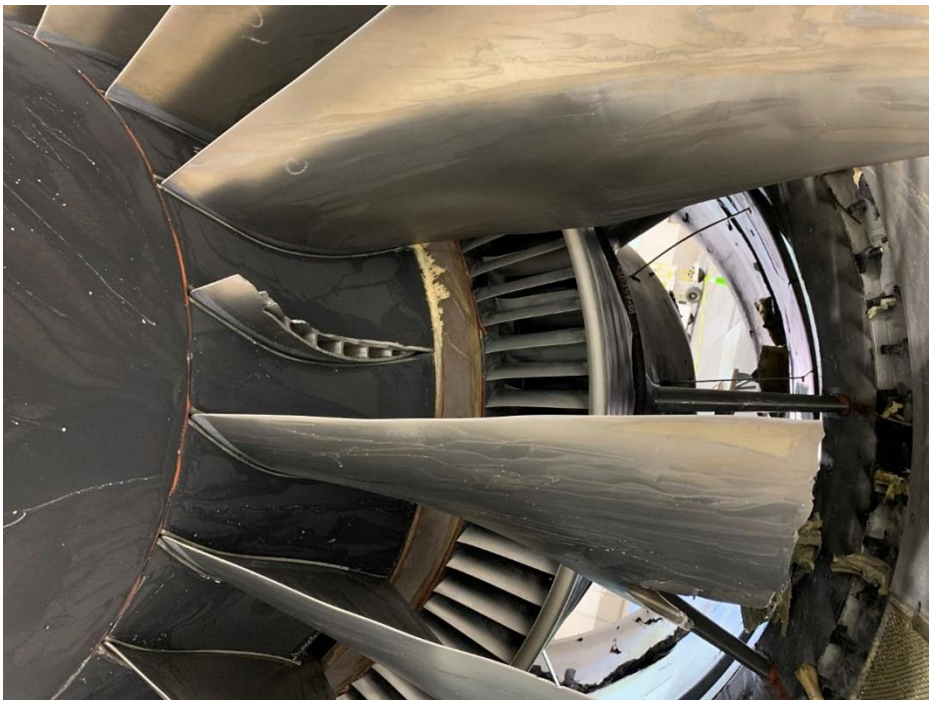

Figure 1: Two fractured blades on the right engine [1]

Metal fatigue is a process that occurs in metallic objects where deformation and failure can occur well under the material's loading limits. This process weakens the metal due to repeated stresses. Think of a thin metal wire; to fracture it would need a significant force, but an alternative method to break the wire is repeatedly bending back and forth. The larger the bends, the faster the wire brakes; this is analogous to the stress's amplitude. This bending force itself cannot break the wire, but over time the metal weakens due to the repeated stress and begins to fail causing a fracture. During the repetitive process, micro-cracks form, concentrating in corners and other stress concentration features. Over time these micro-cracks grow and eventually lead to rapid crack propagation, ultimately leading to failure. Metal fatigue is considered one of the most dangerous failure modes due to the difficulty of detection compared to its risk of catastrophic failure. More generally, these engine failures are caused by hollow fan blade internal crack propagation from cyclical loads and can cause massive damages and loss of life. Figure 2 shows a fan blade where the cracks formed around a stress concentration point.

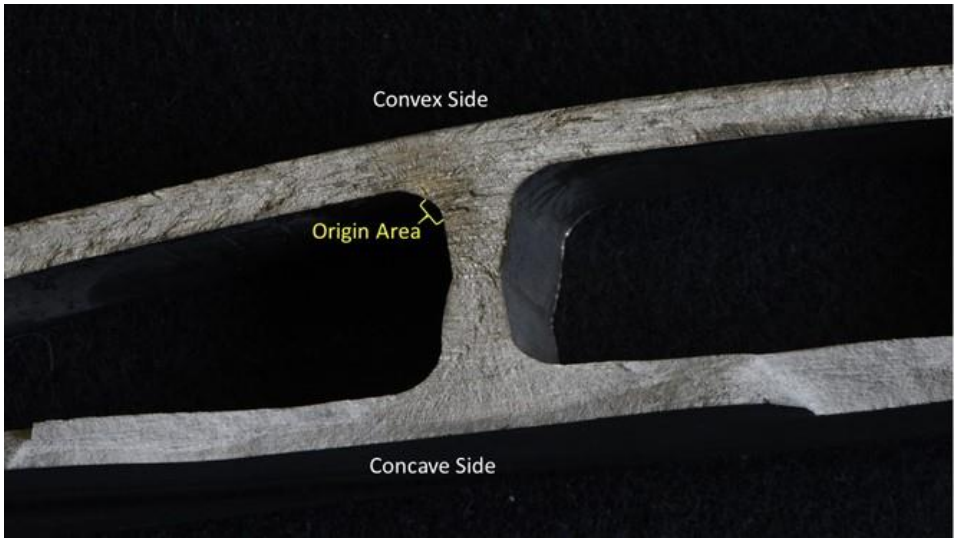

Figure 2: Hollow fan blade fracture surface area [1]

A key way to prevent these incidents is to understand the material limits of components. Fatigue testing is performed to understand material limits better. Fatigue testing enables a better understanding of how a specific material or shape reacts to cyclical loads. These tests enable the collection of data on crack growth and fatigue life or even to validate the safety of certain structures affected by fatigue. Fatigue testing can lead to an understanding of when to inspect materials for signs of fatigue as it may not be noticeable otherwise. Moreover, this allows for proactive repairs and replacements that can save money and lives before incidents occur.

HCF testing, a subset of fatigue testing, occurs in the range of 10^5 to 10 million cycles while applying desired strain or stress rates. Fatigue testing is hugely time intensive as compared to typical metal failure testing. For example, even if a test was operating at a high frequency of around 100 Hz frequency, a 5 million cycle test would require around 14 hours. Generally, high-cost machinery, such as electrodynamic/piezoelectric shakers, are required to engage in HCF testing. Thus, performing testing is both time and cost-intensive.

This project aims to develop a low-cost alternative to the traditional equipment used in fatigue testing. The system's design involves accessible components, can be adapted to many use cases and can be scaled up and down with ease. The testing rig shown below is primarily made up of an AC motor, a VFD motor speed controller, and an eccentric cam mechanism to convert rotational motion into linear actuation. The premise behind this testing rig is to create simple construction of cheap and accessible components to generate a fixed actuation distance. The system drives a test coupon near its structural resonance to generate the target strain amplitudes needed for HCF testing. The main difference between the proposed system and a shaker is the method of adjusting the strain rate. With the shaker, the strain rate is adjusted by the amount of displacement/force

applied to the armature. With the piston motor configuration, the strain amplitude is adjusted by changing oscillation frequency since the piston displacement is fixed. This frequency control allows the increased displacement of the specimen as it approaches resonant frequencies.

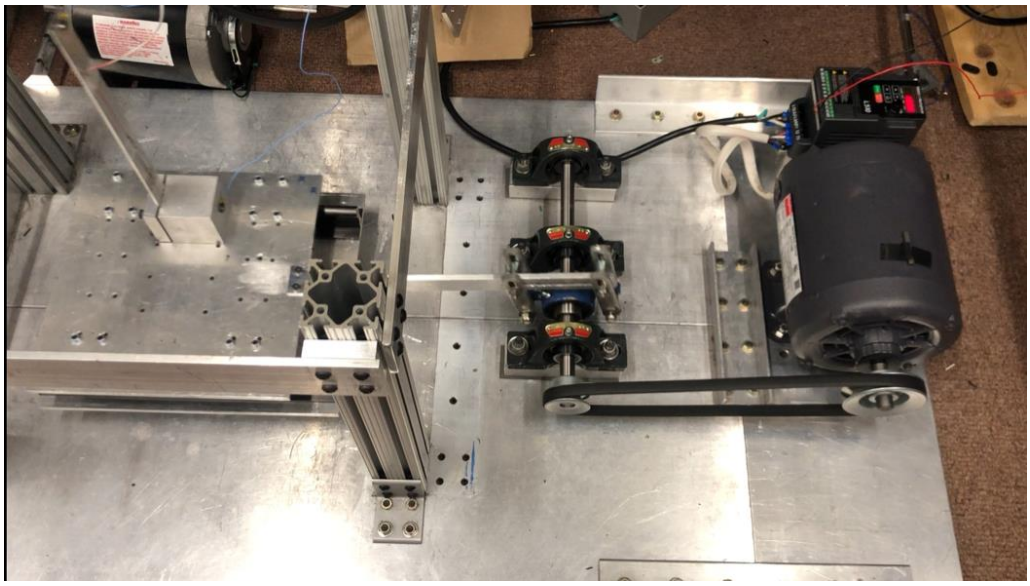

Figure 3: Testing rig

The system also offers the opportunity to incorporate additional control systems such as autonomously reacting to crack formation events. These features allow the system to run without much supervision, which would be needed with more traditional systems.

CHAPTER 2: BACKGROUND

2.1 Fatigue Testing

Fatigue testing is used to understand the material limits in regards to deformation and crack formation. High cycle fatigue testing deals with large cycle counts and elastic deformation, compared to low cycle fatigue testing dealing with plastic deformation with higher stress levels. As cyclical loads are applied to materials, fatigue cracks can form and propagate. Fatigue testing can be used to gather information about a specimen's crack growth properties to ultimately determine the fatigue life; or how long it takes for the specimen to fail. This project is focused on finding an alternative method to conduct HCF testing. Traditionally fatigue testing is carried out on machinery such as servo-hydraulics, shakers, rotating bending machines, and ultrasonics. [2] Each system offers its own advantages to certain types of testing. From [3], the most basic requirements for a strain-controlled fatigue testing system are:

- the ability to continuously apply cyclical loads for long durations until specimen failure
- the ability to indicate total accumulated cycles
- the ability to consistently impose strain within target strain limits
- the ability to control strain amplitude
- measurement devices for analysis and control

This project aims to develop an alternative to these machines to create a lower-cost testing system compared to the current methods. This project aims to achieve the goal of applying constant or variable amplitude HCF testing with the ability to stop testing when a failure definition is achieved. This project is only aimed at small-scale specimens or coupons.

2.2 Forced Vibrations and Resonance

The natural frequency of an object is the frequency said object oscillates at when struck without consideration to damping or a continuous force application. This can be express as $\omega_n = \sqrt{\frac{k}{m}}$, where k is the stiffness and m is the mass. In the application of HCF testing, the system is in the presence of both damping and a forced oscillation; Damping through the material itself and other mechanical system components; And forced oscillation as the driving force to induce cyclical loads. The resonance frequency describes the frequency when a system experiences increased amplitudes as the driving frequency approached the system's natural frequency. This is due to the forcing frequency occurring in-phase with the natural frequency allowing for compounding amplification of the driving force. This can also occur at around multiples of the natural frequency referred to as first, second, third, etc. modes. For most cases, the first or fundamental mode is of the greatest concern as it has the largest amplitude increase. The level of damping present in the system can change the resonance frequency. When measuring the input and output of a system, a frequency response can be obtained to understand the system's characteristics. This allows the finding of the system's resonant frequency at the largest amplitude peaks. In relation to this project, the changing amplitude around resonant peaks can be leveraged to increase or decrease the strain amplitude. This allows for a control method based on driving frequency rather than driving force.

[4] explores different methods of characterizing response curves of single degree of freedom (SDOF) systems. Two of the methods stand out as being useful in this project to determine frequency response constants — using phase and frequency measurements or using stress and frequency measurements. These methods result in the statements that "The damping may be

determined from the ratio of π to the amplification factor A" or that "the damping may be determined directly from the tangent of the phase angle for which the exciting frequency has either 1.62 or 0.62 the value of the natural frequency multiplied by π." Bernhard provides numerical examples for each of his methods. These methods could be useful for verifying the constants determined by other methods or could be implemented into an adaptive updating controller for constants.

2.3 AC Motor Control

AC motors are generally built to operate at a single speed regardless of the voltage applied, contrary to DC motors. AC motor speed is dependent on the frequency of the power supply. In order to control the speed of an AC motor, a process would be needed to alter the frequency of the motor input voltage. Variable Frequency Drives have been created to accomplish this task. There are various types of VFDs for different input and output power requirements; by far the most common is the AC to AC with DC-link VFD. This type of VFD works as follows "rectification of fixed frequency, smoothing and then inverting to give variable frequency to feed an a.c. machine" [5, p. 91]. The rectification works by first converting the AC power to DC through a converter using diodes. The DC power is then smoothed through the use of capacitors. Then the DC power is modulated and inverted back to AC using an arrangement of controlled transistors. Pulse width modulation techniques are used to match the V/Hz ratio for constant torque rated for the motor [5, pp. 91-99]. Common VFD control types are V/f, vector, and flux vector. These types have different operating characteristics. For example, the controllable speed range could vary from 10%-100% to 0%-100%, and the ability to regulate speed between 3% and 0.001% of the motors rated speed [5, pp. 473-476]. A big factor to consider is matching the VFD specifications to the motor

specifications, mainly VFD power output to the motor power input, the rated horsepower, and the rated speed.

2.4 Closed-Loop Feedback Control

When controlling a process variable such as strain amplitude, feedback control is necessary in order to stabilize and converge on a target value. In regards to HCF testing an open-loop controller could be used to control the strain amplitude, but this would require previous knowledge of the system dynamics to run at the target strain amplitude for a set amount of time/cycles. A more adaptable approach would be to develop a closed-loop feedback controller. This controller could begin testing on an unknown material and, over time, adjust to the target setpoint through feedback corrections. Feedback loops incorporate controllers in order to correct the signal based on sensor feedback. Two useful control strategies available are PID control and model predictive control (MPC). PID controllers are some of the most commonly used controllers for their effectiveness and ease of use. This will be the main source of control in the controller design. PID controllers work by applying error correction based on gain values of the proportional, integral, and derivative terms. The proportional term accounts for the current error and is a large corrector when the difference between the setpoint and the measured process value is high. The proportional term allows the reduction of rise time and steady-state error, but if the gain value is too high, it runs the risk of overshoot and instability. The integral term sums error over time and corrects for that accumulation. The integral term, similar to the proportional term, reduces rise time and increases the likelihood of overshoot; the benefit comes from eliminating the system's steady-state error. The derivative term applies a damping correction related to the rate of change of error. The derivative term decreases overshoot and settling time of the system. Gain tuning is the method of

adjusting the PID terms' gains to improve system performance. The Ziegler-Nichols method of tuning a PID controller is the simplest and most common. This method can be used to develop an initial tuning based on the ultimate gain, which can later be fine-tuned if additional performance is needed [6, pp. 196-209]

Due to the simplicity of the system, MPC methods shouldn't be necessary but could provide an option for future expansion for crack detection events and on-line parameter adjustment. For the PID controller, due to the system's time scales, relatively small gain values will be used, and the extra complexity of the derivative term may be removed, forming a simpler PI controller.

2.5 Adaptive Controllers

A simple PID controller for HCF use may lead to instability as material stiffness changes throughout the test. This becomes even more problematic when cracks begin to propagate as this severely changes the material's properties. [7] implements a method of pretuning the PID controller based on the model of a reduced-order plant transfer function. This allows the gains to incorporate material dynamics in the form of physical properties of the material. In order to pretune the initial parameters of the reduced model estimates are made using error least-squares methods. He notes, something important to this project, that additional filtering terms are needed to improve fitting behavior around resonant and low frequencies. Once data is experimentally gathered from a representative test specimen; the model can be fitted using iterative methods. In addition to the pretuning, Clark implements a grey-box adaptive controller to estimate the stiffness of the material to update stiffness terms on-line during testing. He chooses a recursive least squares estimator

(RLS). This could be useful for longer tests where the material has more opportunity to change properties. For most cases the simplest design of a PID controller will be adequate.

CHAPTER 3: MECHANICAL SYSTEM DESIGN

This thesis's primary goal is to design a motor control system to maintain a constant strain amplitude during HCF testing. In order to fulfill that task, a method to convert rotational motion from the motor to translational motion is needed.

3.1 Actuation method

A rig was constructed in order to transfer power with two pulleys and a belt to a shaft with an eccentric cam. A piston arm is attached between the mounted ball bearing and the sliding plate. The sliding plate is guided along low friction bearing rails in a single degree of freedom. On top of the flat plate, a clamp is positioned to secure the testing specimen. The actuation displacement is fixed and is generated through the use of a self-aligning mounted ball bearing. The ball bearing is intentionally tightened unevenly to introduce eccentricity to act as an eccentric cam. As the shaft rotates the self-aligning bearing pitches off axis and introduces a small displacement through this action. As the shaft rotates the pitch oscillates back and forth to introduce a fixed cyclical displacement provided to the piston arm.

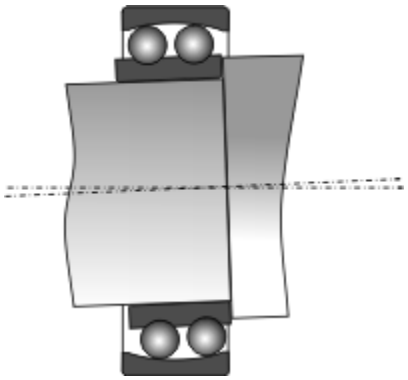

Figure 4: self-aligning ball bearing, (creator: Lidingo)

The testing rig in Figure 5 used in this project needed to be modified as the rig was initially constructed for different purposes. This required machining new mounting holes in the aluminum pieces to hold the new motor and for a new sliding plate assembly configuration.

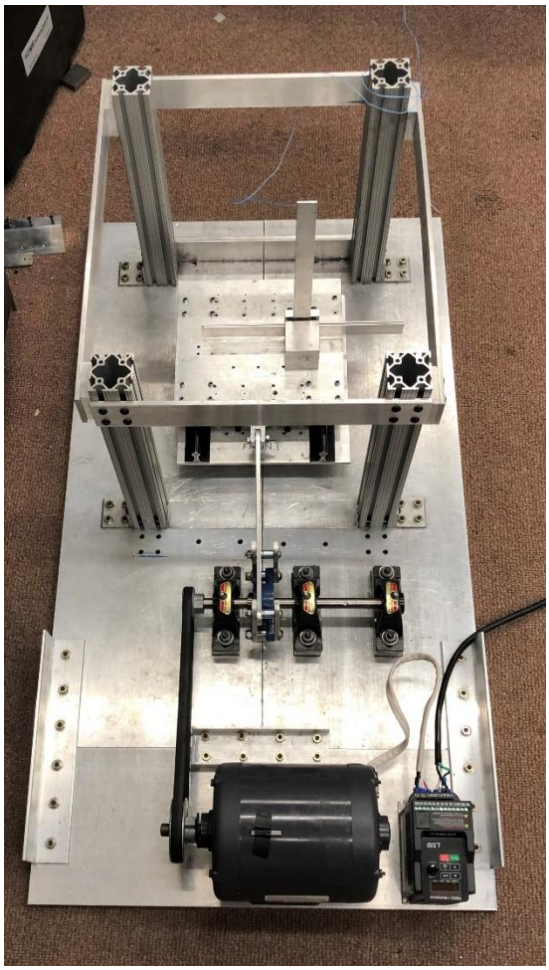

Figure 5: HCF testing rig

A future development to improve the actuation method could be to use an overhung rotor system to introduce displacement. At higher speeds, the ball bearing introduces additional off-axis transverse oscillations (as compared to axial displacements) that can affect the ability to cleanly

transmit a specified frequency. An overhung rotor could fix this issue by fixing the transverse displacements to only allow for axial displacements.

3.2 Component Selection

3.2.1 Motor and Controller

The method to control the motor's frequency depends on the selection of an AC or DC motor. The main advantages of DC motors are the ability to provide high torque at zero speed. This is an unnecessary requirement for the application of a motor in this system, and thus does not justify the increase of cost for a DC motor. A 3-phase 230V, ½ horsepower, 1725 RPM AC motor was selected due to the mechanical system's requirements. The 1725 RPM allows the motor to operate above the 3% speed (1 Hz) range, where slowing the motor too much could lead to overheating. ½ horsepower is adequate to provide the power to actuate the pully system and is a typical motor power that allowed for more options.

To control an AC motor's frequency, the use of a variable frequency drive (VFD) is needed. A sensorless vector control AC-DC-AC VFD was selected due to its increased speed regulation capabilities of around ±0.2% of max frequency as compared to ±2% for scalar V/f Control [8]. This will allow more refined control of oscillation frequency. As the frequency approaches resonance, small changes can have significant effects on the amplitude of oscillation. The VFD specifications were matched with the AC motor selected, mainly compatible voltage, phase, and horsepower. The VFD takes input power from common USA wall power single phase 115VAC and converts it to 3 phase 230VAC, which the motor accepts. The types of materials planned for

testing need to be kept in mind for the motor and VFD pairing speed range to reach resonance frequencies adequately.

3.2.2 Pulleys

In order to properly transfer power from the motor to the piston shaft, a series of pulleys were needed. Two pulleys were selected; one smaller with an outer diameter of 1.75 inches attached to the shaft and a larger one with an outer diameter of 3 inches attached to the motor. This leads to a gear ratio of 3:1.75, which allows us to reach higher frequencies if needed. The ratio allows an output frequency 1.714 times larger than the input resulting in a speed range of ~ 1-50 Hz.

3.2.3 Measurements

Two methods were used to conduct measurements. A laser doppler vibrometer was chosen as a method to measure displacement and velocity values as it was a part of the lab's equipment. In addition, piezoelectric accelerometers were used to gather acceleration data. The accelerometers were attached to the mounting clamp and the beam's furthest end to measure input and output acceleration data, as seen in Figure 6.

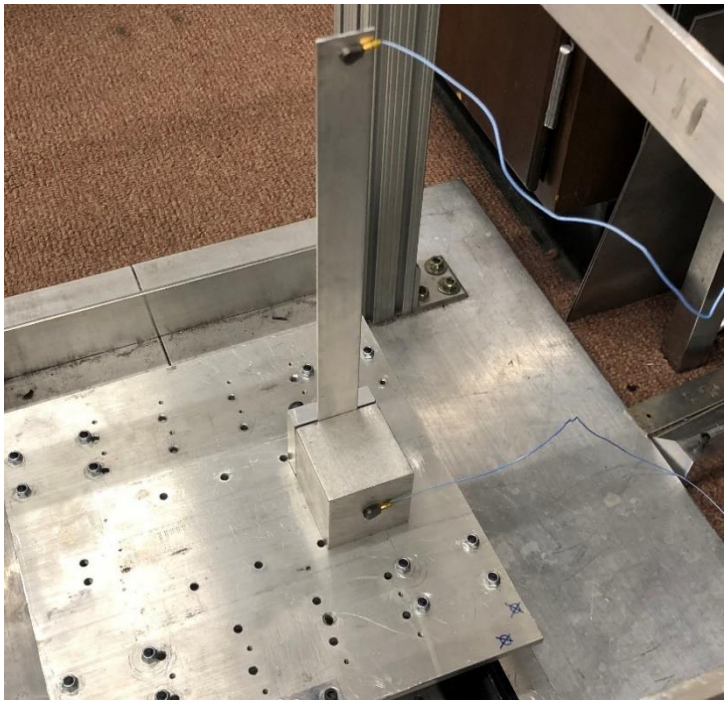

Figure 6: accelerometer mounting locations

3.2.4 Data Acquisition

An NI CompactDaq chassis is used along with the C series voltage input and output modules to transfer voltage signals between the vibrometer, LabVIEW, and the VFD. An updating frequency of 5 ms is adequate for this project and the long time scales planned. If higher updated frequencies are needed, a real-time measurement system can be substituted.

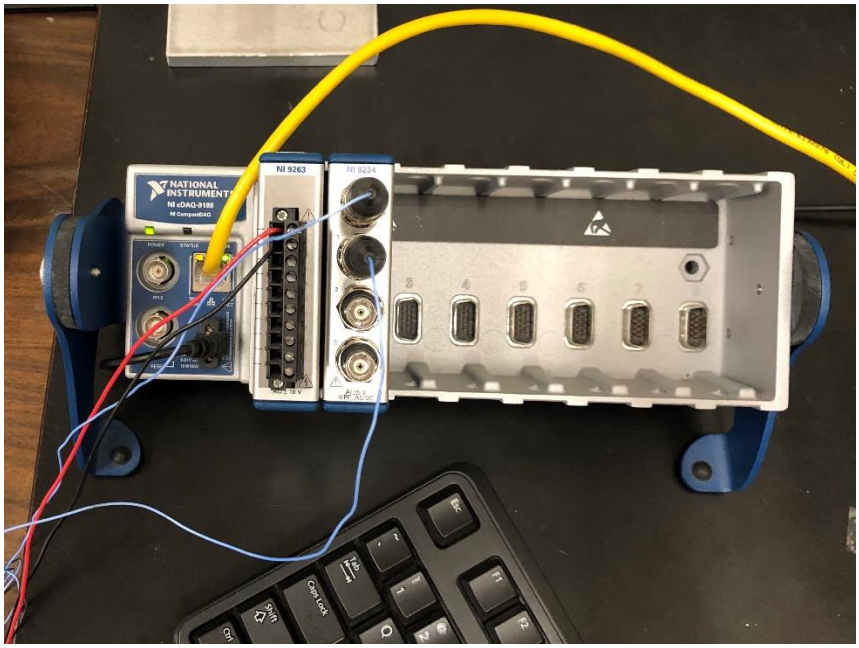

Figure 7: data acquisition setup

3.3 Component setup & verification

The VFD has a setting for an external analog voltage input to set the frequency of the drive. To verify that the VFD operated nominally, readings from the onscreen display were taken at voltage intervals from a variable power supply.

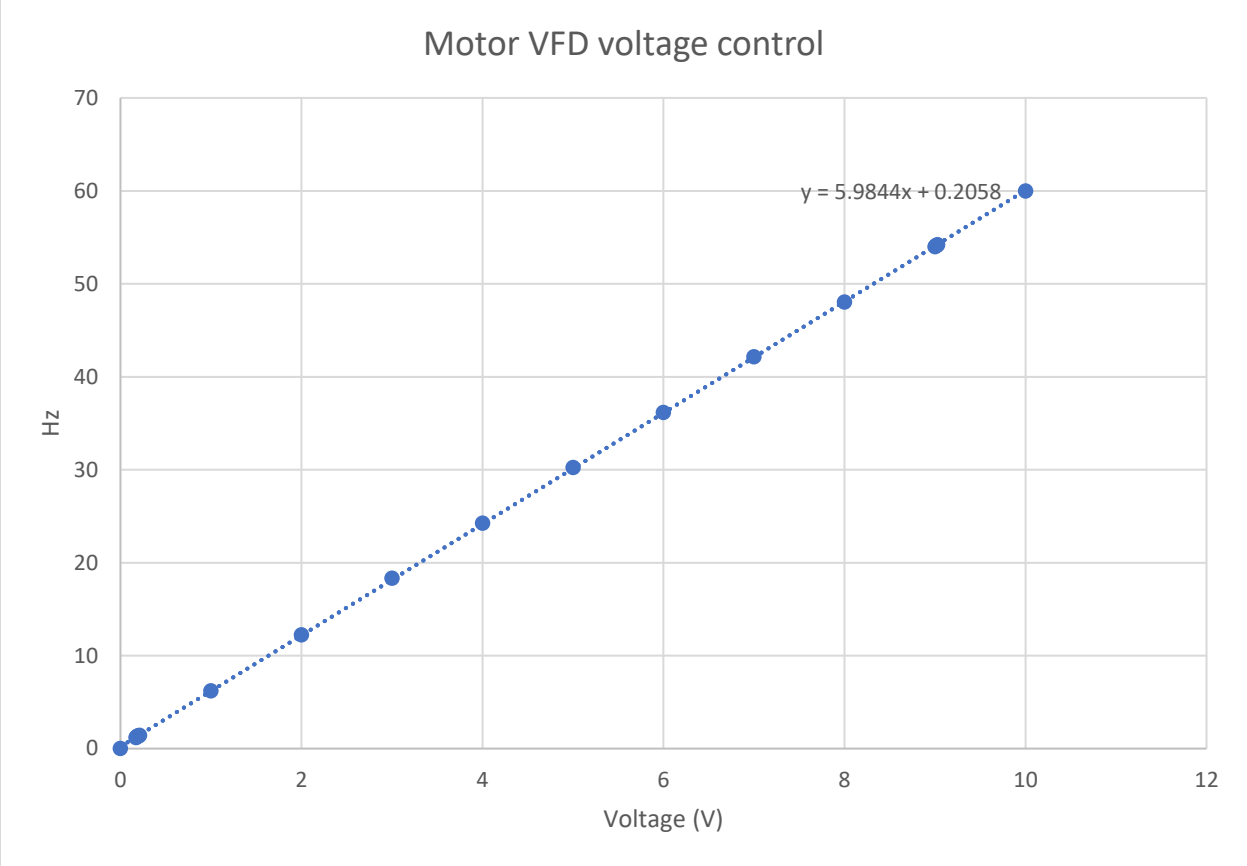

Figure 8: VFD analog input verification

It can be seen in figure 1 that the Analog inputs result in a linear response where each voltage responds to 6 Hz. This would lead to a VFD that has frequency control from 0-60 Hz.

In order to further verify that the VFD is actually outputting the correct frequencies to the motor, we need to measure the motor rotation rate. The laser vibrometer was aimed at a padded small metal plate lying against the motor shaft that was heavily damped. The laser would measure the plate's velocity as the motor's shaft bumped the plate when the keyed portion raised it. These velocity readings were then run through a Fourier transform to find the dominant frequency and were saved.

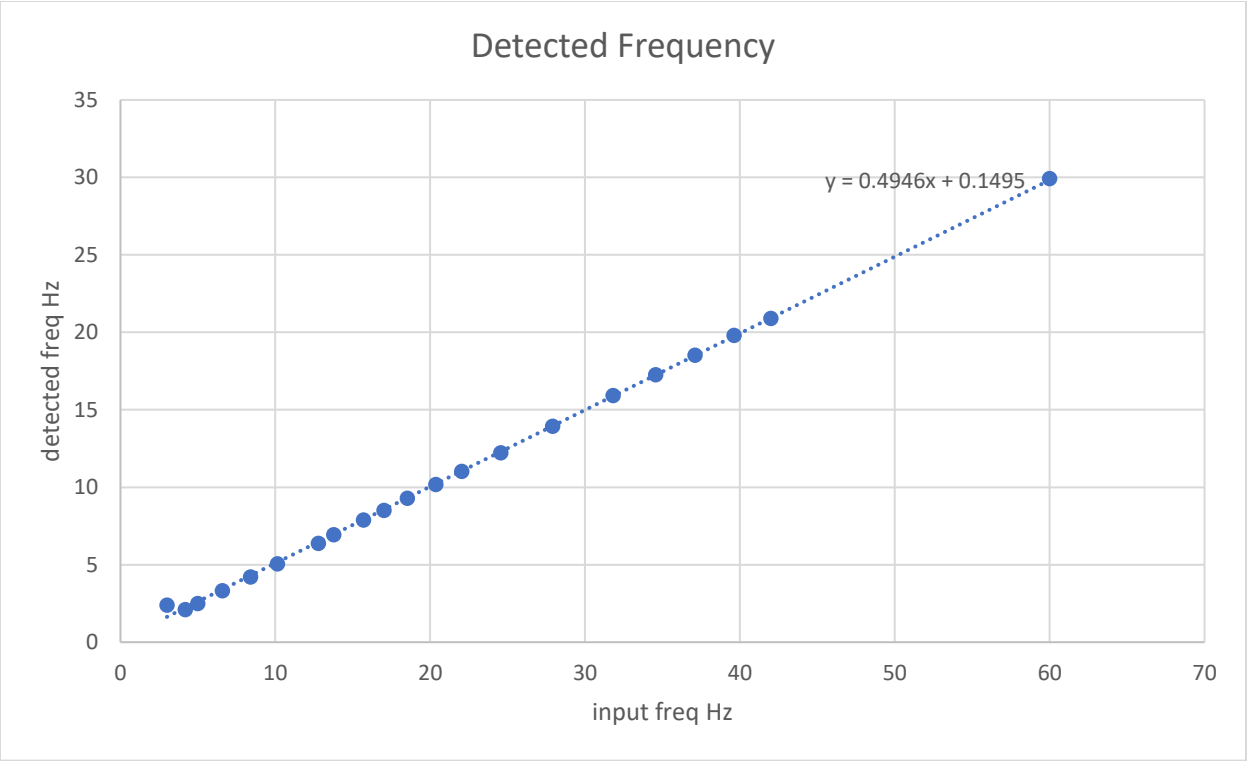

Figure 9: Detected output frequency

As shown in figure 2, the VFD controlled the motor to half the frequency as expected. This leads to a limited output frequency from 0-30 Hz. While this was a surprise, this was still adequate for the purposes of this project. The main concern is fine control of the frequency changing over time. Also, the input to output follows a linear relationship which allows for easier control. As the materials we are testing have a relatively low first-order resonance frequency of ~10 Hz, the system can output a max frequency of 51.428 Hz with a gear ratio of 3:1.75.

CHAPTER 4: CONTROLLER DESIGN

The method to do so is to manipulate motor frequency to approach the material's resonant frequency. Adjusting the frequency will change the oscillation amplitude, which in turn will increase or decrease strain amplitude.

4.1 System Dynamics

When deriving a reduced-order system, the driving system (the motor, pulley system, and piston) is collapsed to simplify modeling. This allows the system to be modeled as an SDOF system. The specimen is considered to have an internal stiffness and damping.

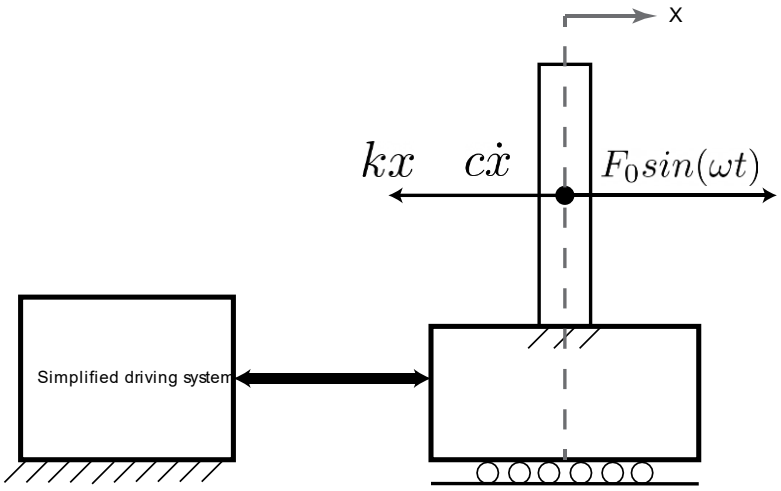

Figure 10: reduced-order system diagram

This system's differential equation of motion is

$$\ddot{x} + \frac{c}{m}\dot{x} + \frac{k}{m}x = F_0 \sin(\omega t) \qquad (4\text{-}1)$$

where $\frac{c}{m} = 2\zeta\omega_n$, $\frac{k}{m} = \omega_n^2$. From [9] phase angle (ϕ) and amplitude (X) can be solved for.

$$\phi = \tan^{-1}\left(\frac{2\zeta(\omega\backslash\omega_n)}{1-(\omega\backslash\omega_n)^2}\right) \quad (4\text{-}2)$$

And

$$|X(\omega)| = \frac{F_0/k}{\sqrt{[1-(\omega\backslash\omega_n)^2\,]^2 + [2\zeta(\omega\backslash\omega_n)]^2}} \quad (4\text{-}3)$$

The equation of the frequency response function can be determined through curve fitting algorithms to estimate the modal parameters. From [10] and [7] different estimation tools are discussed, the most simple being rational least-squares estimation.

4.2 Material Characterization

The main objective in determining material characteristics is to experimentally define modal parameters such as the resonance frequency and damping ratio. A quick estimation of the 1st mode cantilever beam resonance frequency can be made using (4-4). Solving for an aluminum beam of length 10 inches and area 4.032e-5 m^2; where E is 68.9 GPa for aluminum, I is 8.468e-12 m^4 for the beam; where $\beta_1 L = 1.875$ for a cantilever beam. The estimated 1st mode frequency solves to $f_1 = 20.077$ Hz

$$f_1 = \frac{(\beta_1 L)^2}{2\pi}\sqrt{\frac{EI}{\rho A L^4}} \quad (4\text{-}4)$$

Using this f_1 a frequency sweep can be used for a range of frequencies around the 1st mode. Two accelerometers were affixed to the testing specimen (Figure 6): first fixed on the clamping base to

act as an input, the second to the specimen's tip to act as the output. These two acceleration measurements can be used to form an acceleration transmissibility function. This would ultimately enable the determination of modal parameters. A range of 1-30 Hz was determined to encompass the estimated resonant frequency with an adequate buffer. While traditional Frequency sweep methods would employ a chirp function, The VFD accepts a voltage value to drive a specific frequency to the motor. To run a frequency sweep on the VFD motor system a series of voltage steps would be needed, which can be seen in the top right of Figure 11.

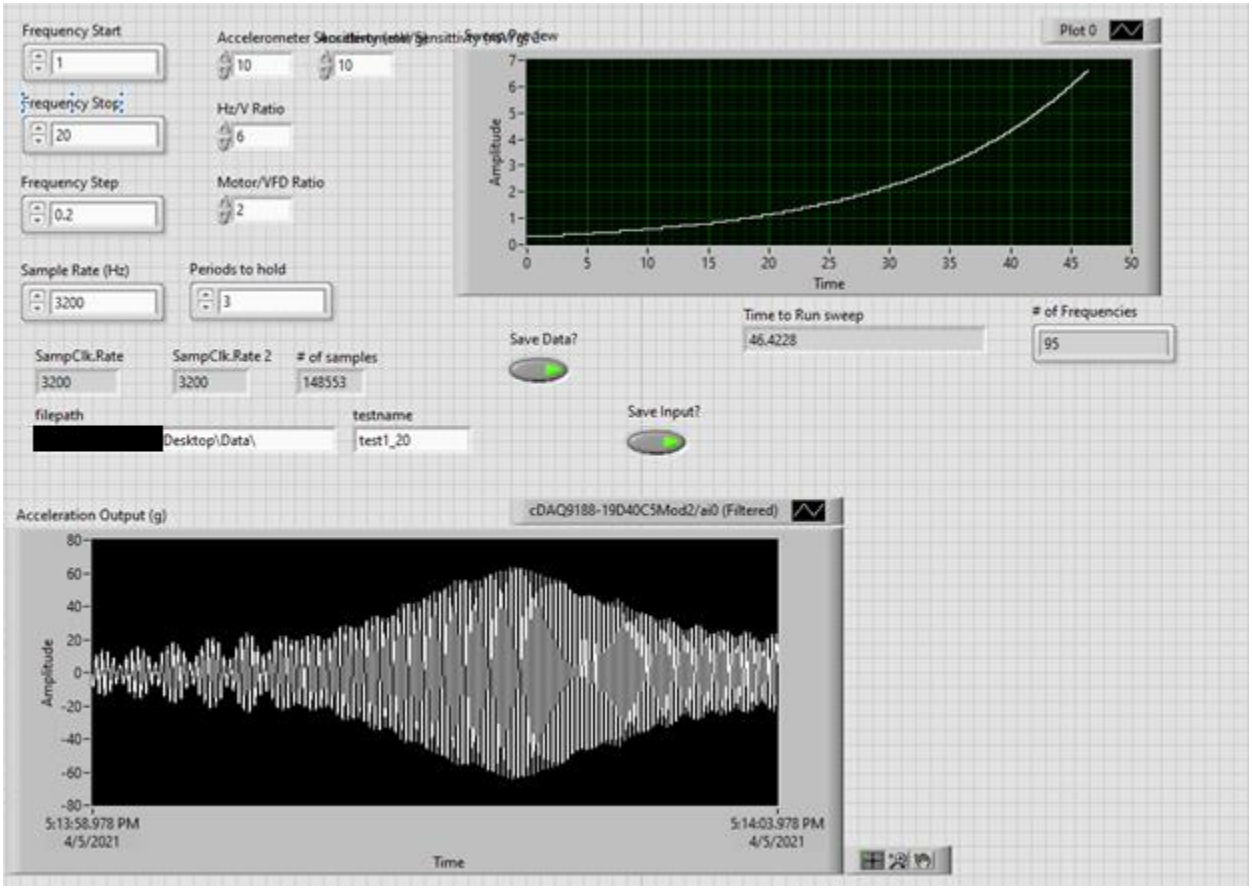

Figure 11: Frequency sweep VI front panel

A LabVIEW virtual instrument was created to populate an array with the voltage signal values required for this sine sweep, as seen in Figure 12. The amount of time a particular signal remained was dictated by its associated period. A hold time of 5 periods was chosen as a base to reduce transient effects while reducing the overall sweep time. For example, a 1 Hz signal, with a 1 second period, would be held for 5 seconds. And a 5 Hz signal for 1 second. Increasing the length of this period hold time would increase the frequency response's accuracy as it will reduce the transient effects of previous frequencies. To account for the signal transmission conversions, a V/Hz ratio of 6 was used from Figure 8, and a gear ratio of 1.714 was used.

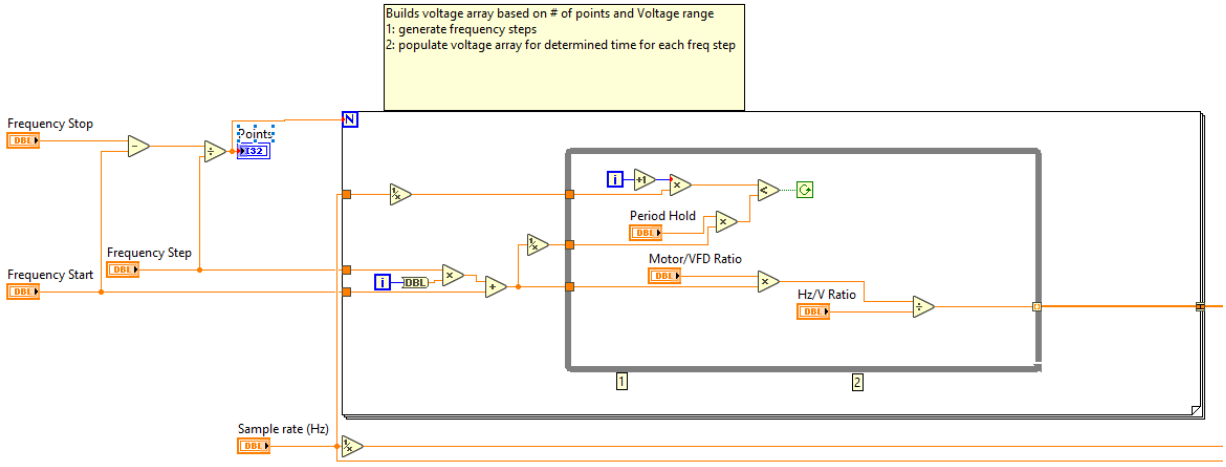

Figure 12: Frequency sweep signal generation

This was deemed adequate for the experimental verification of the material characteristics. An additional method to minimize transients effects could be to approximate an exponential sweep function using polynomial curve fitting and outputting that curve to reduce the impact of harsh steps in frequencies.

The data acquired shown in Figure 13 shows the output (tip) acceleration in the top plot and the input (base) acceleration in the bottom plot. As time moved forward, the frequency was incremented higher. A fairly steady increase in magnitude can be seen in the input acceleration. The output acceleration was fairly constant until it approached its first mode resonant frequency, where the amplitude increased drastically, as expected from a resonant response.

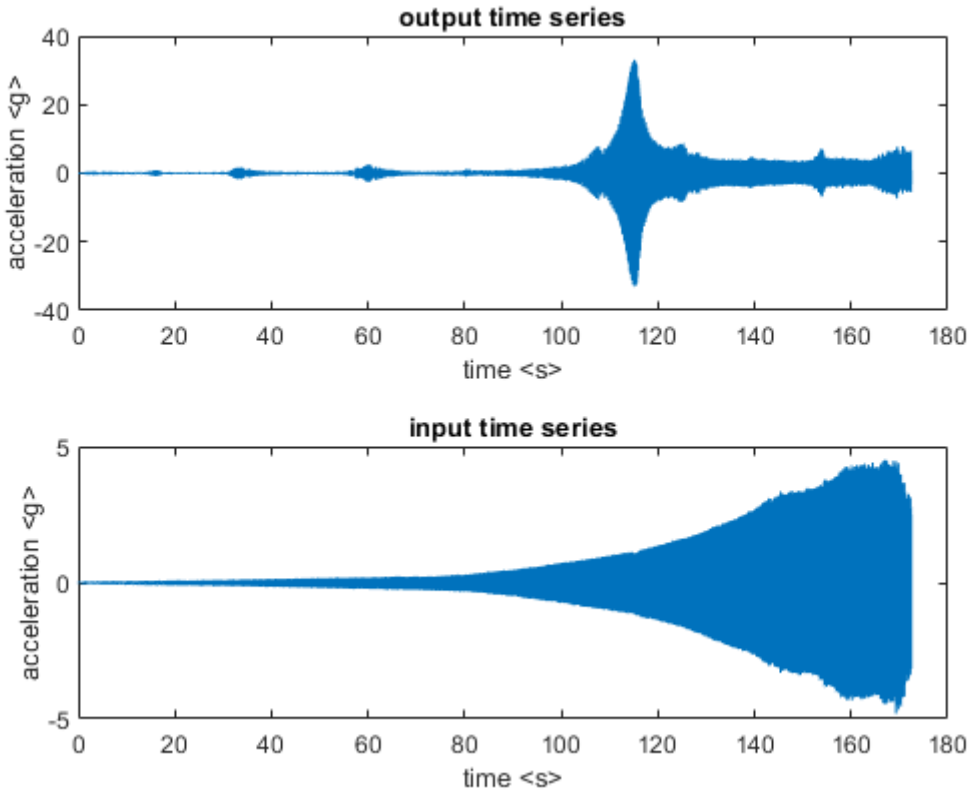

Figure 13: Frequency sweep time-series data

The time-series data was then converted into the frequency domain utilizing a discrete Fourier transform (DFT). The FFT function in Matlab was used to produce the single-sided frequency domain plots seen in Figure 14. This shows the frequencies and their relative amplitudes

throughout the sweeping test. It can be seen that the peak in acceleration magnitude shown in Figure 13 corresponds to the peak in Figure 14. This peak signifies the system's resonant frequency occurring at roughly 15.15 Hz.

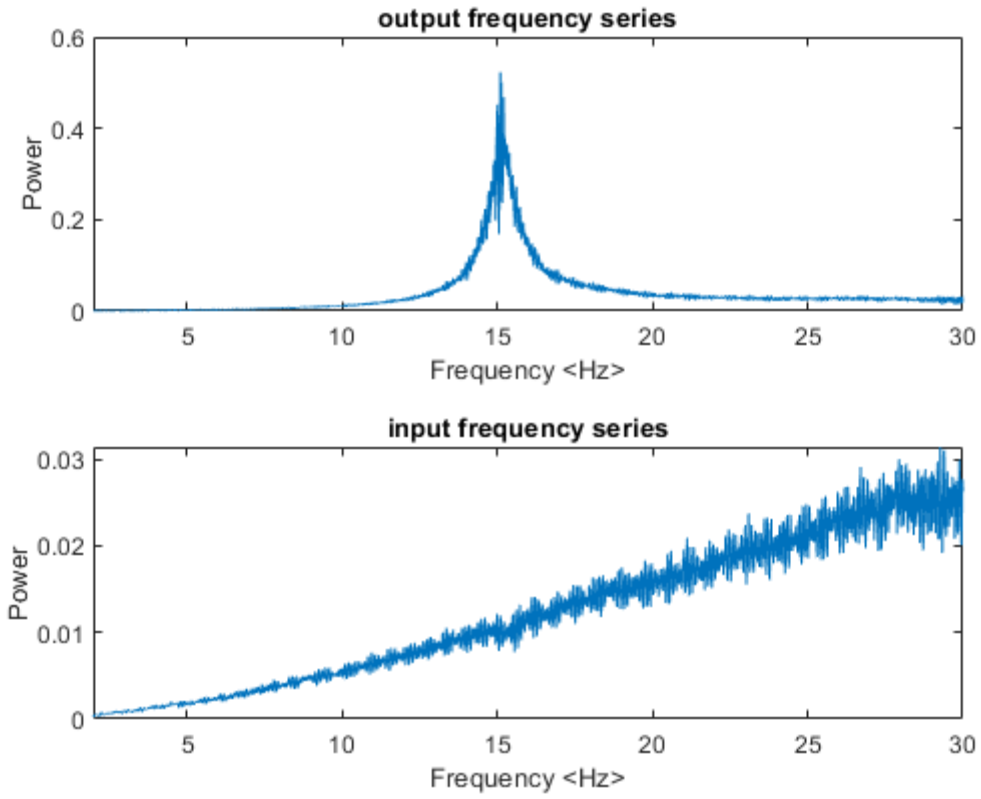

Figure 14: Frequency sweep FFT plots

When dividing the output frequency series by the input frequency series, the transmissibility function can be obtained. Phase information from the function can be found using (4-2) finding the inverse tangent of the imaginary portion divided by the real portion. Using the function a Bode plot can be constructed, as shown in Figure 15. The phase data addition allows for another indication of the resonance frequency when it crosses the -90 degrees phase. The small spike in

phase data near 21 Hz is likely due to noisy data as the phase data was filtered through a threshold where it may have exceeded the limit and was not considered 0. This spike is unimportant in the analysis of the material.

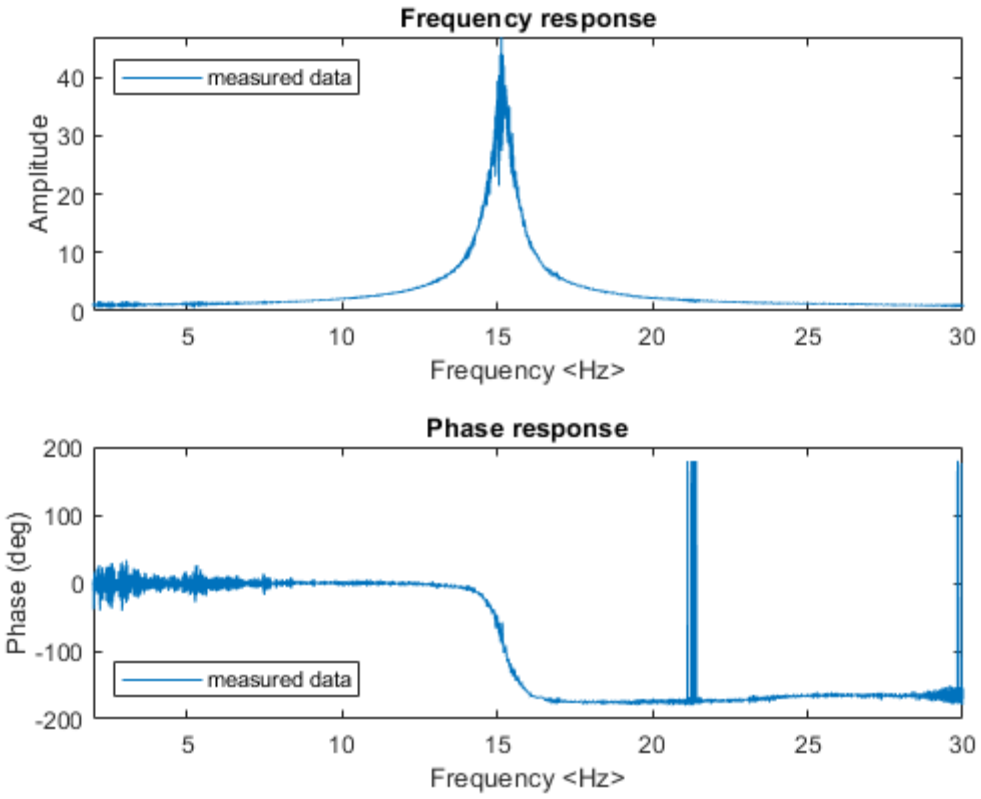

Figure 15: Frequency response function Bode plot

Next, there are multiple methods for determining modal parameters from the data. The first is to directly observe the Bode plot. The first mode resonance frequency is where the peak occurs at 15.15 Hz. Using the half-power method described in [11, p. 314] equation (4-5) can be used to find the damping ratio, where $f_1 = 14.97$ and $f_2 = 15.265$ are the half power response frequencies given by the resonance peak magnitude divided by the $\sqrt{2}$ on either side of the peak. The damping ratio ζ can be approximated to be 0.0098.

$$\zeta = \frac{(f_2 - f_1)}{2f_r} \quad (4\text{-}5)$$

Or if assuming small ζ equation (4-6) from [12, p. 2_36] shows the peak magnitude value in terms of ζ for transmissibility functions.

$$\text{Peak Magnitude} = \sqrt{1 + \frac{1}{4\zeta^2}} \quad (4\text{-}6)$$

The damping ratio can be approximated to be 0.0107 using this method.

The second method to determine modal parameters is to curve fit the transfer function. MATLAB was used to estimate a transfer function using the tfestimate function; The function uses Welch's averaged periodogram method. But many curve fitting methods, such as using the rational fraction polynomial method would yield similar results. The tfestimate function approximated a transfer function in the S domain with the values $\frac{342.1}{S^2+0.6133S+231.2}$. Using the denominator in conjunction with (4-1), the coefficients can be used to determine modal parameters. The 0^{th} order coefficient 231.2 can be set equal to f_r^2, leads to an $f_r = 15.206$. The 1^{st} order coefficient 0.6133 can be set equal to $2\zeta f_r$, this leads to $\zeta = 0.0201$. The modal parameter results are tabulated in Table 1.

Table 1: Modal parameters

	f_r	ζ
Half power method	15.1543	0.009759
Transmissibility Peak Magnitude	15.1543	0.010671
Transfer function curve fitting	15.2066	0.020165

The estimated value of the 1st mode frequency from (4-4) is in close proximity with the measured data. The differences in values could be a combination of material defects and differences along the beam, in addition to the testing system characteristics which could influence the resonance of the beam. The different methods are overlayed onto the measure data in the plot below. The plot observation techniques better capture the near resonance "peak" amplitudes. In comparison, the curve fitting approach better estimates the overall contour. Of course, gathering better-behaved data may lend to closing the difference between the various methods. These different methods lead to the possibility of switching transfer functions to have a more accurate estimate based on proximity to the resonance frequency.

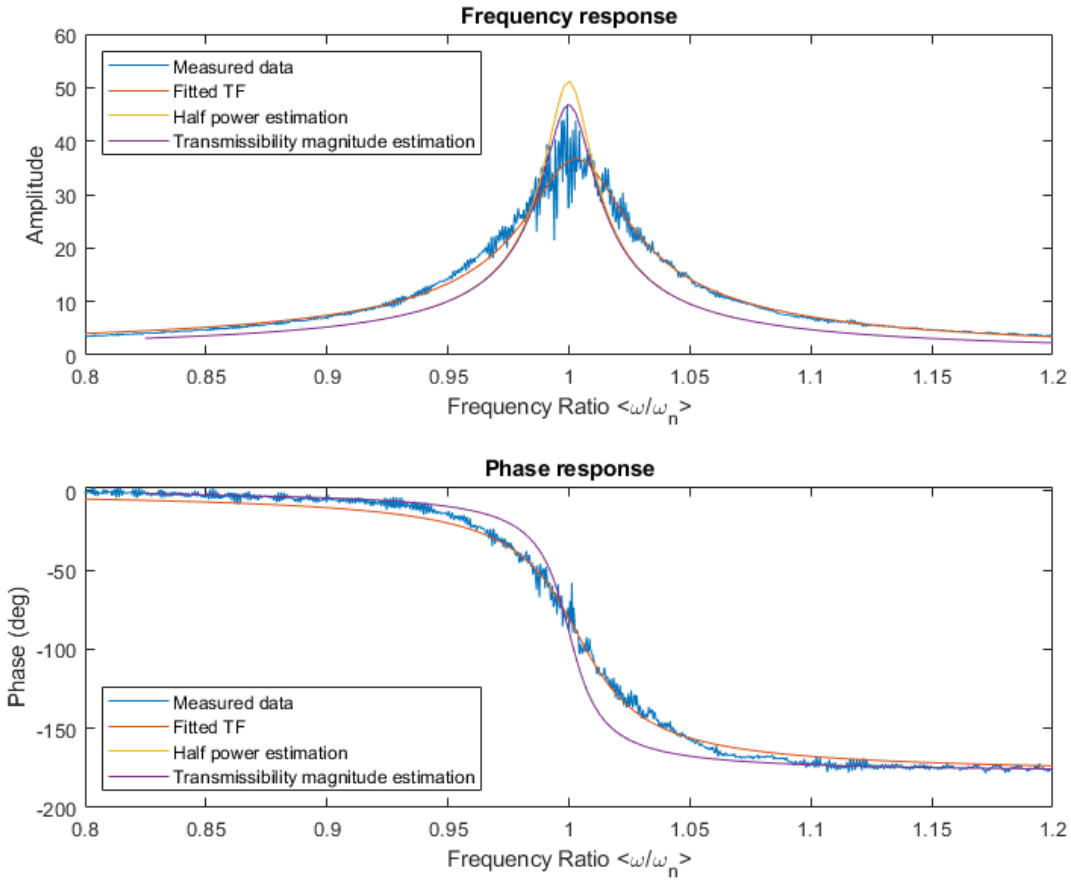

Figure 16: Transfer function estimations

4.3 Controller methods

The controller method to be implemented is a PID controller. Known for its effectiveness and simplicity, this controller can fit the needs of the system. A Labview VI was created to implement a PID controller shown in Figure 19. The inputs to the system were reading acceleration from the tip and base and strain values. These inputs are then filtered using a bandpass filter with a 1-60 Hz range to reduce noise outside the testing frequency ranges. The PID controller process variable can

be set to a frequency, acceleration amplitude (input or output), or strain amplitude. Since the input is oscillatory by nature and not constant readings, the values need to be averaged over many cycles to achieve accurate results; without averaging, the signal would be susceptible to noise spikes. Acceleration amplitude was chosen as the process variable during development as it was the easiest to work with, but for the final system, strain amplitude will be used.

To prepare the controller for use with strain, a frequency sweep needs to be run to collect data on strain amplitude at various frequencies similar to the process described in section 4.2 Material Characterization. A new specimen's strain amplitude data is collected in the frequency domain below, along with the input acceleration.

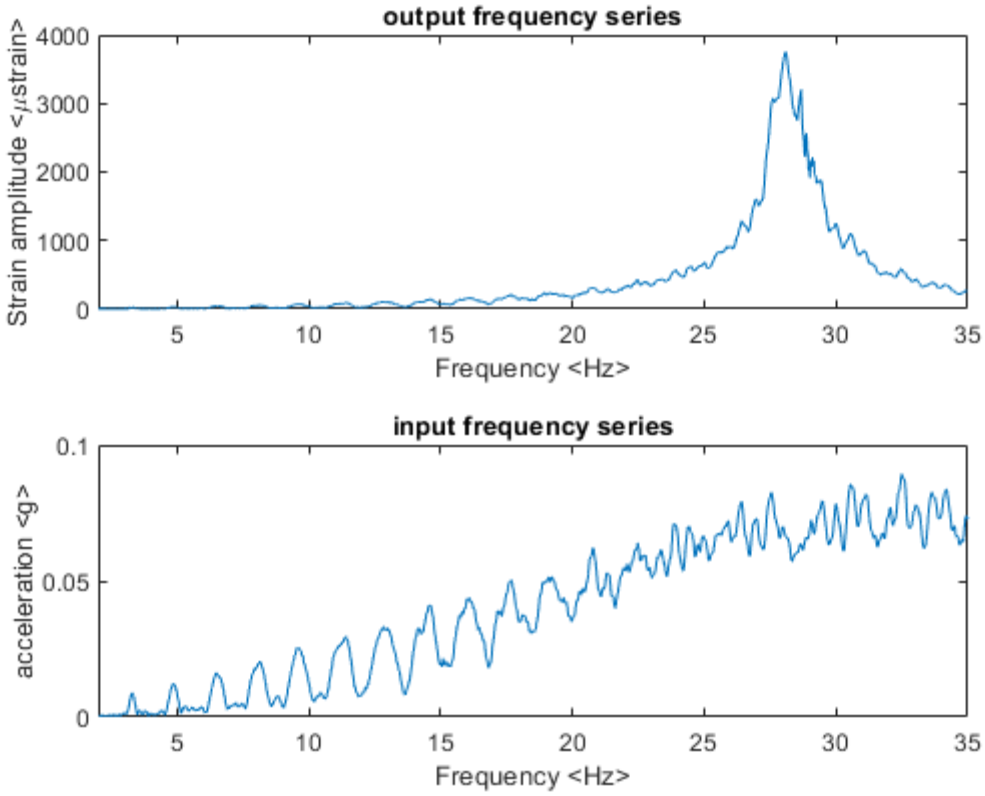

Figure 17: Strain amplitude frequency series

The way the feedback loop operates is by first taking in reading measurements for a specified loop time. This data would be filtered and then subdivided. The number of subdivisions would be calculated based on the input signal frequency, and the number of cycles deemed adequate to get an average. Each subdivision would then be searched for a maximum value, equating to the signal's amplitude for that subdivision, then averaged with all the subdivisions. The averaged value would then be used as the process variable for the PID controller. The PID controller then outputs an update signal in terms of the process variable. In the case of strain, it will be put through a fitted exponential function to the left half resonant curve of the form $a * \exp(bx) + c * \exp(dx)$ where x is the strain amplitude, shown in the figure below.

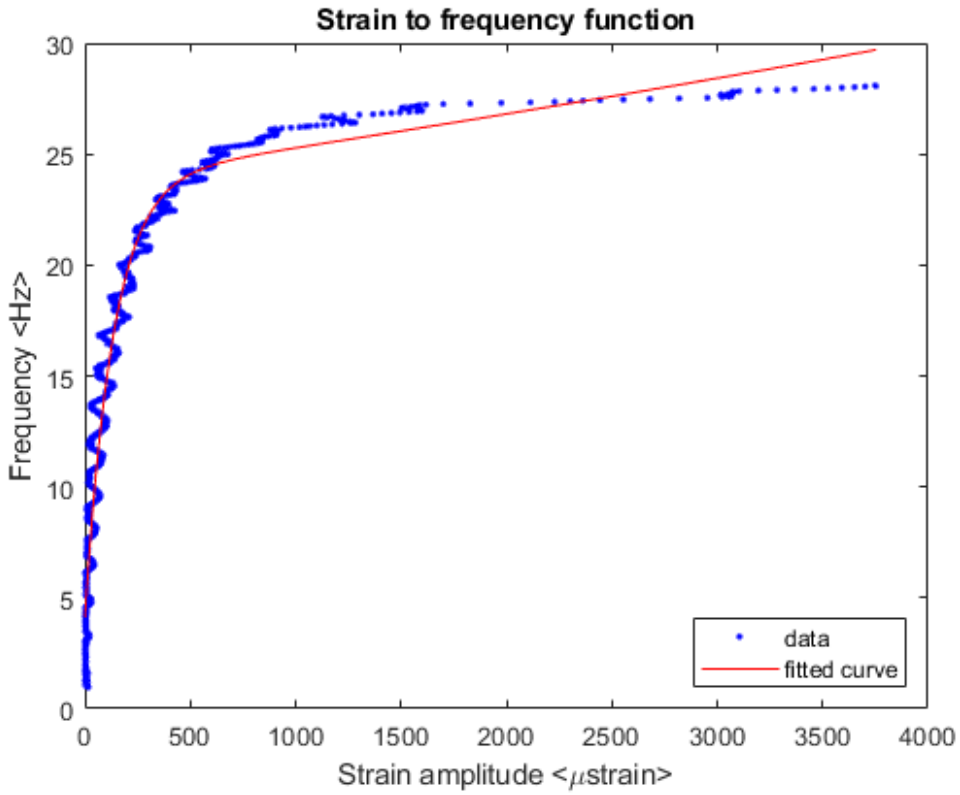

Figure 18: Strain to frequency nonlinear exponential fitting

There are some inconsistencies from the time domain magnitude and frequency domain magnitudes. This could be attributed to spectral leakage where some of the magnitudes is not appropriately captured due to the finite resolution of frequency bins. A minor corrective scaling factor can be used to adjust for this based on the peak magnitude. Overall the fitted curve is just an estimation guide to help the PID controller make more accurate updates. Small inaccuracies don't matter as much as the PID controller accounts for these in the feedback adjustments over time.

Once the strain is converted into frequency, the frequency needs to be adjusted according to the system: first due to the gear ratio and second due to the motor/VFD ratio. Finally, the frequency needs to be converted into a voltage with the V/Hz ratio so that the VFD can accept the signal. Since the reading signals are being captured in blocks determined by the loop time, the PID update can only be written after each loop time. The limit for the loop time is theoretically limited by one cycle, but this could lead to noisy data and inaccurate adjustments which will be discussed in later sections. In application, since the loop timing is based on software, loop timings less than 5 ms may be unattainable unless hardware-based timing solutions and real-time systems are used. These limits posed do not interfere with the project goals, as HCF testing is based over long periods, and the speed of the controller is less of a concern.

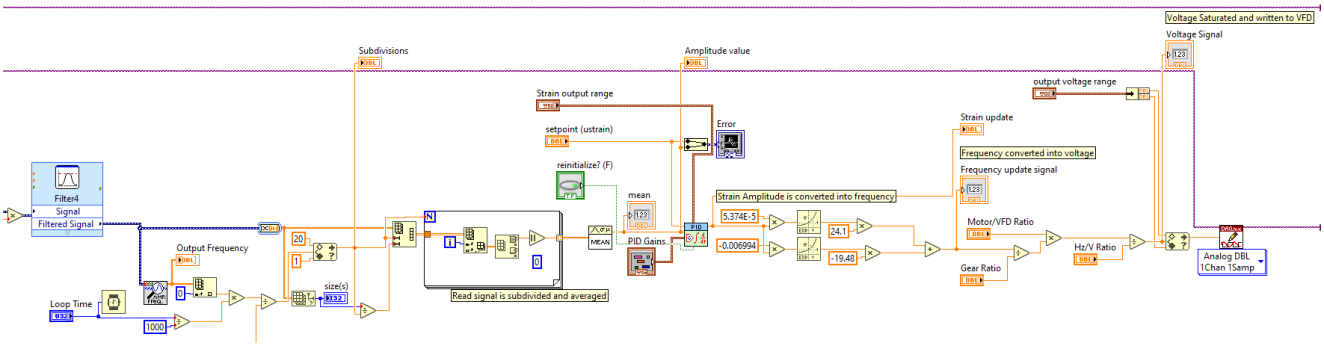

Figure 19: PID controller VI back panel

4.4 PID controller tuning

Multiple methods can be pursued when tuning A PID controller; one of the more popular methods is the Ziegler-Nichols Tuning method. But since this is a highly experimental process, the trial and error method was chosen to adjust the gains. The goal of the controller should be to emphasize stability over speed. As the transient effects from harsher updates could remain in future readings causing instability. The gains should be relatively low to prioritize stability. The integral term should also be low for the long loop times being read, which could drive up the integral term's weight. The derivative terms inclusion is used to help increase the system's stability by minimizing overshoot and oscillations.

CHAPTER 5: RESULTS

5.1 Methods

The testing specimen is first placed in the mounting bracket to see how much length is held within the clamp. A spot is then marked for attaching a strain gauge. The marked area is then sanded down and wiped with isopropyl alcohol to smooth and clean the area for secure adhesion. The strain gauge is then glued to the prepared area and allowed to cure.

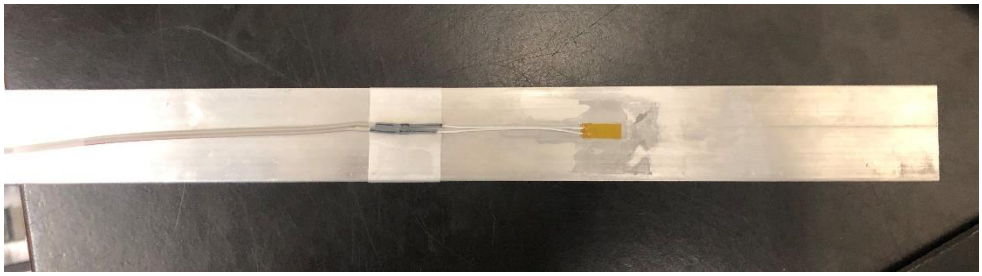

Figure 20: Specimen with a strain gauge attached

Once cured, the specimen is then placed back into the clamping mount, and the accelerometers are attached to the base and tip, as shown in Figure 6. The strain gauge is then connected to a Wheatstone bridge connected with a similar unused strain gauge. The wires are then directed into the cDAQ slots based on input. Wires are then routed from the output card to the VFD external voltage control slots. In total, there are two acceleration inputs, one strain input, and one voltage output from the cDAQ mounting bracket. Once the connections are set up, run a frequency sweep and collect the data for the process variable in the frequency domain. Fit a second-order exponential function to the data to allow for conversion from the process variable to frequency.

The LabVIEW VI for the PID controller is then loaded; in the back panel, update the exponential fit coefficients shown in Figure 21 with the values obtained from fitting in Figure 18.

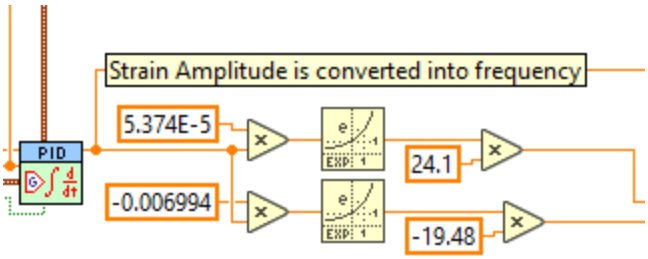

Figure 21: Exponential fitting coefficients

As shown in Figure 22 the options for the PID gains, loop time, target setpoint, output voltage limits, and measurement sensitivities are available to modify. The top plot shows the Process variable and setpoint plotted against time, while the graph below outputs sensor readings.

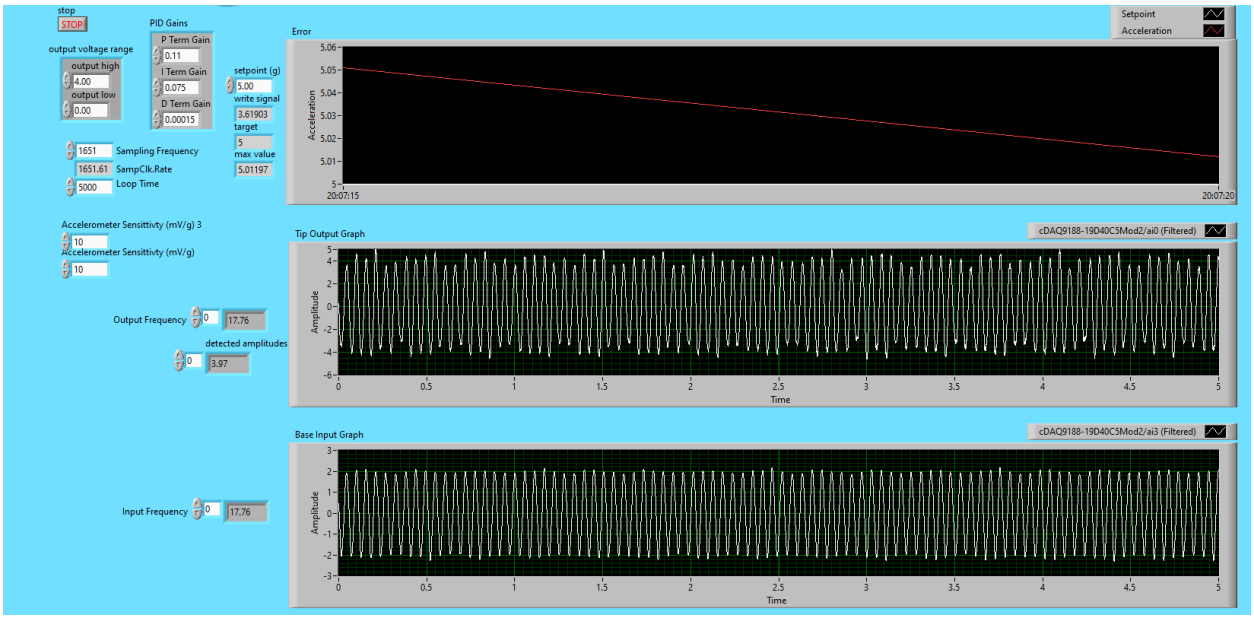

Figure 22: PID control front panel

5.2 Material testing

5.2.1 Acceleration amplitude testing

Acceleration was taken as the process variable for the initial testing as the data was more well behaved and less noisy. The PID values listed in the table below were found to be ideal gains for acceleration as the input. The proportional term was found by slowly increasing until slight oscillations occurred. The I term was slowly increased to help speed up reaching minimal steady-state error. The derivative term was then increased to a point where it lowered the oscillation to increase stability.

Table 2: Acceleration PID values used

K_p term	T_i term	T_D term
0.01	0.075	0.00033

The next option to hone in on is the feedback loop time. Lowering the loop time increases the update rate and feeds the controller less accurate data due to noise. Also, the more times the frequency is updated, the more transient effects are read in future signals making the data less accurate, as seen in Figure 23. Lowering the loop time causes more frequency disturbances, making corrections happen before the signal can even out, essentially feeding in less precise data. The acceleration amplitude can be seen to have a lot more oscillation and instability approaching the setpoint. Using 500 ms loop time takes approximately 30 seconds to reach the target value, and 2 minutes to reach the setpoint value; it still oscillates a fair amount and never settles down.

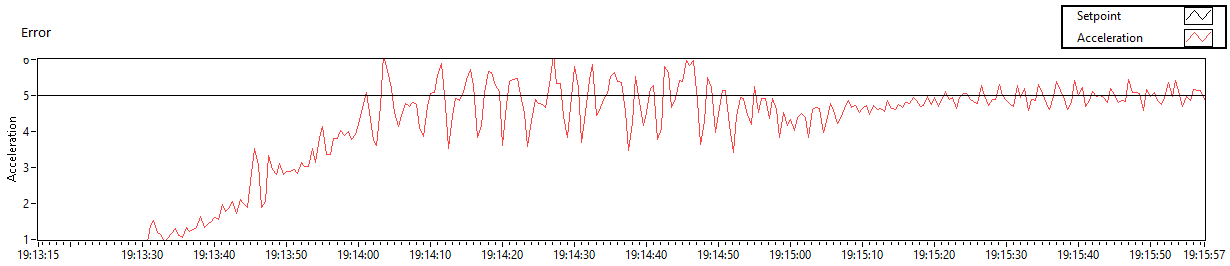

Figure 23: 500 ms loop time

Changing the loop time from 500 ms to 2500 ms allows significantly more data to be captured and more time for the transient frequency change effects to wear out seen in the figure below. It takes 25 seconds to reach the target value and settles down in 77 seconds with some slight instability

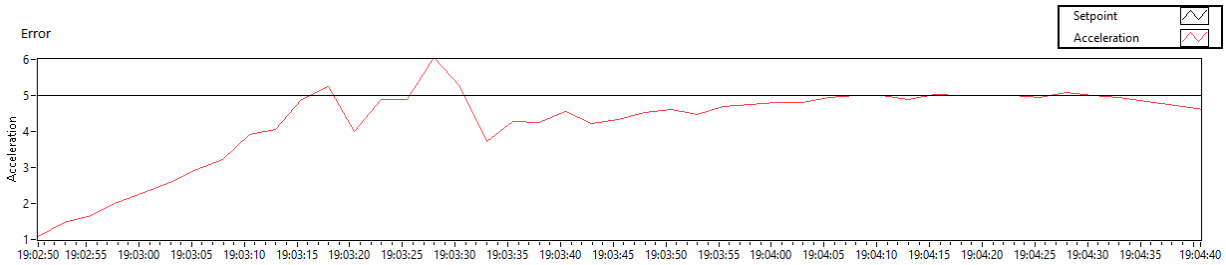

Figure 24: 2500 ms loop time

Changing the loop time from 2500 ms to 5000 ms has a much smoother transition. It takes 58 seconds to reach the target value; while it takes longer to reach the setpoint, it immediately settles when it reaches. This selection has minimal overshoot and is very stable with slight oscillation on the steady-state error, as seen in Figure 25. The 5000 ms loop time leads to a nice sweet spot between lowering transient effects and smoother transition without taking too long to reach the set

value. This loop time also leads to stability when the setpoint is reached since the values are averaged over longer periods of time with greater subdivision.

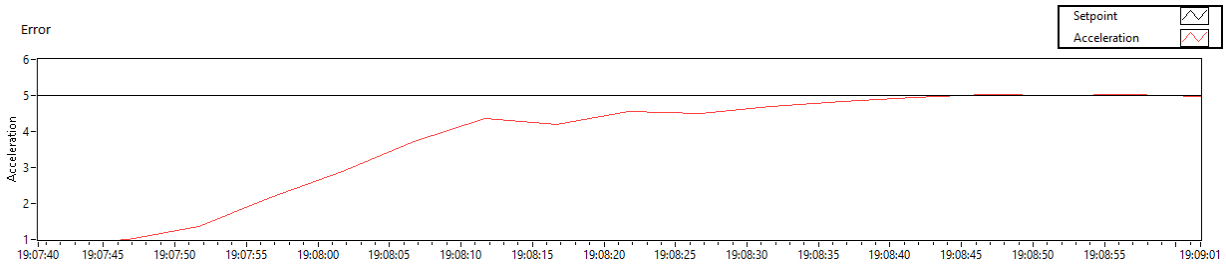

Figure 25: 5000 ms loop time

5.2.2 Strain amplitude testing

After understanding the process from the acceleration testing, strain values were used as the process input. These readings were more noisy and sensitive than the acceleration values, so the controller's stability will be slightly less than that of acceleration. A loop time of 5000 ms was chosen for these tests as this was the longest loop time LabVIEW could handle in memory with a sample rate of 1651 Hz. The following plots show various PID controller terms' performance, where their respective values follow P, I, and D in Figure 26. Their performances are as follows:

(a) takes 23 seconds to reach the target value while slowly lowering the steady-state error with some minor fluctuations

(b) raising the P and I terms and lowering the D term from (a) takes 26 seconds to reach the target value with some small overshoots but overall less steady-state error as time continues

(c) lowering the P and I terms and raising the D term from (a) takes longer to reach the target value after some corrective dips at 66 seconds. These values seem to have the least oscillation once

the controller settles but not much performance gain over (b), taking nearly three times as long to reach the target value.

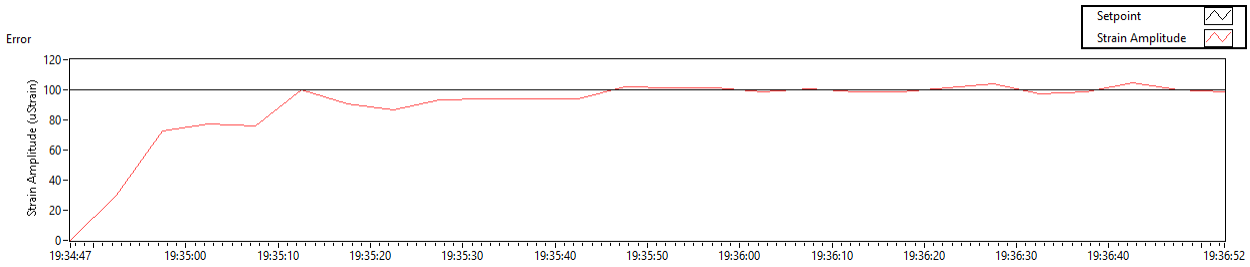

(a) K_p = 0.5, T_i = 0.05, T_d = 0.0005

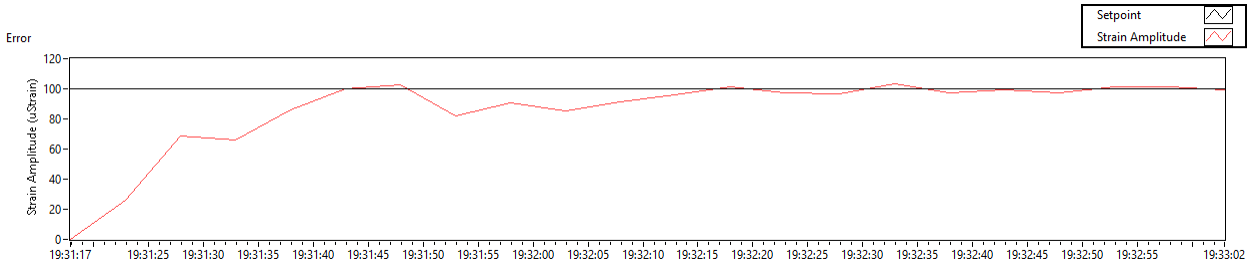

(b) K_p = 0.55, T_i = 0.06, T_d = 0.0003

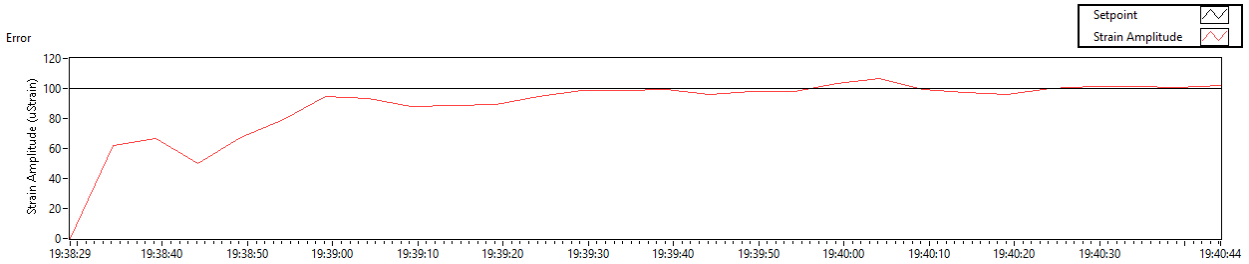

(c) K_p = 0.45, T_i = 0.047, T_d = 0.00054

Figure 26: 3 different PID controller performance plots

CHAPTER 6: CONCLUSION

Through this research, a low-cost system has been developed to enable HCF testing. A fixed displacement — variable strain amplitude system was created by combining accessible components such as an AC motor, VFD, an eccentric cam. This was made possible by taking advantage of the material's resonance and a feedback controller to change the frequency required for target strain rates. The controller design utilizes a PID controller with tuned gains based on the process variable. The controller also incorporates material characteristics determined from a frequency sweep. The PID updates are fed through a fitted exponential function that estimates frequencies required to obtain that update value. Through hours of discontinuous testing, the system has reached well over an estimated 250,000 cycles, proving its capabilities over high cycle counts.

When looking at the Strain amplitude testing, the optimal controller setting is found in Figure 26 (b) with proportional, integral, derivative terms: 0.55, 0.06, 0.003, and a loop time of 5000 ms with a sampling rate of 1651 Hz. These lead to good controller performance, with 23 seconds required to set target values while settling in under a minute. Due to the long time periods required for HCF testing, a faster controller is unnecessary, especially at the expense of stability.

6.1 Discussion

The results shown in chapter 5 lead to the realization that longer loop times, while they update slower, offer superior stability when dealing with oscillatory process variable inputs. This is especially true for specimens with low damping as transient effects continue to linger, causing input data to be a mix of multiple impulse frequencies interacting.

Additionally, many variables can be used as the controlling variable for HCF testing; It was shown in chapter 5 that acceleration shows better controlling performance than the strain measurements. As long as the characterizing frequency sweep is collected with the controlling variable planned along with strain, a conversion can be set up to take advantage of a more favorable and accurate measurement method.

6.1.1 Limitations

Due to the fixed displacement design, the system is limited by the specimen attached. The highest possible strain rate is limited by the strain amplitude available at the resonant peak. So careful consideration should be given when planning to use higher amplitude testing. For example, with one of the testing specimens used, the highest available strain amplitude was 2,114 $\mu strain$ given at the resonant frequency. If higher values are needed, a possible solution is to increase the system's fixed displacement to transmit more energy into the specimen.

Since the resonant peak is approached exponentially, instability issues are possible when using frequencies very close to the resonant peak. To operate close to the peak, a highly tuned system and model need to be selected to precisely control the strain amplitudes. Another possible solution, similar to the previous limitation, is to change the fixed displacement to operate at a more favorable frequency range on the resonant curve.

6.2 Future research

This thesis was created in the span of two semesters. Given more time, additional research would be devoted to the following areas, as these topics could increase the system's effectiveness.

6.2.1 Stiffness Estimator

An on-line stiffness estimator could be beneficial for particular specimens and tests. Material more prone to plastic deformation could update stiffness value as the material properties change over time to maintain an accurate record of what is happening within the material. This could also lead to a faster, more accurate adaptive controller. The methods discussed in [7] could be used for future improvement.

6.2.2 Model predictive control

While the current feedback controller incorporates material characteristics, the implementation still leaves more to be desired as it is still entirely reliant on the PID controller tuning. Further research could be devoted into developing a more accurate model of the material system combination. This would allow for model predictive control (MPC) as the primary feedback mechanism, with a secondary PID controller to correct for slight changes or model discrepancies.

6.2.3 Overhung rotor

The current method of converting the motor’s rotational motion to linear actuation is an eccentric bearing. The advantages are discussed in 3.1 Actuation method. This would require redesigning the systems shaft and connection mechanisms, But would ultimately lead to an improved system as the overhung rotor would lessen undesirable off-axis vibrations resulting in a cleaner transmission of frequency to the specimen.

REFERENCES

[1] O. o. A. Safety, "United Airlines Flight 328 Boeing 777 Engine Incident," NTSB, 2021.

[2] S. Stanzl-Tschegg, "Very high cycle fatigue measuring techniques," *International Journal of Fatigue*, vol. 60, pp. 2-17, 2014.

[3] *Standard Test Method for Strain-Controlled Fatigue Testing*, ASTM International, 2020.

[4] R. K. Bernhard, "Determination of the Static and Dynamic Constants by Means of Response Curves," *Journal of Applied Physics*, vol. 12, no. 12, pp. 866-874, 1941.

[5] B. Drury, The Control Techniques Drives and Controls Handbook, London: The institution of Engineering and Technology, 2009.

[6] G. F. Franklin and J. D. Powell, Feedback Control of Dynamic Systems 7th ed., Pearson, 2015.

[7] D. W. Clarke, "Adaptive control of materials-testing machines," *Automatica*, vol. 33, no. 6, pp. 1119-1131, 1997.

[8] S. Peterson, "How to Choose the Right Control Method for VFDs," Machine Design, 23 10 2014. [Online]. Available: https://www.machinedesign.com/motors-drives/article/21833844/how-to-choose-the-right-control-method-for-vfds. [Accessed 2020].

[9] W. T. Thomson and M. D. Dahleh, Theory of Vibration with Applications 5th ed., Pearson, 1998.

[10] R. J. Allenmang, "Experimental Modal Analysis and Dynamic Component Synthesis," Air Force Wright Aeronautical Laboratories, Cincinnati, 1987.

[11] D. Eqins, Modal Testing: Theory, Practice, and Application, England: Research Studies Press LTD., 2000.

[12] C. W. d. Silva, Vibration and Shock Handbook, Boca Raton: CRC Press, 2005.